Numerical simulation of gas-solid two-phase flow in a two-dimensional horizontal channel with sudden expansion

Mofreh H. Hamed
Mechnaical Power Eng. Dept., Faculty of Eng., Menoufiya Unversity, Egypt

Gas-solid turbulent two-phase flows and interaction between gas and particles phases in a horizontal two-dimensional channel with sudden-expansion have been studied by numerical simulation using a modified k-ε model. The turbulent fluid flow is governed by Eulerian approach, whereas the particulate flow is governed by the Lagrangian trajectory equations. The mutual effects of the solids on the gas-phase, (two-way coupling), are taken into account. The effects of flow Reynolds number Re, mass loading ratio m_R, channel height ratio H_o/H_i and particle diameter, D_p on the flow behaviour and particles trajectories were also investigated. A fully developed inlet flow conditions was assumed, while all the particles have been introduced in the flow with approximately the same fluid bulk velocity. Comparisons are made with present predicted results and others published experimental and numerical data for both phases and a reasonable agreement is obtained. The results show that the behaviour of gas-solid two-phase flows in a horizontal sudden-expansion channel is affected greatly by flow Reynolds number, particle diameter, height ratio, and mass loading ratio. In addition the particle trajectories are also affected by recirculating flow regions especially particles of small diameter, small inlet height and low velocity.

تبحث هذه الورقة دراسة السريان الاضطرابى ثنائي الطور لغاز وجسيمات صلبة خلال قنوات أفقية ذات اتساع مفاجيء باستخدام. تأسس هذا النموذج النظرى العددى بمحاكاة السريان خلال هذه القنوات مستخدما معادلات أويلر لسريان الغاز الاضطرابى وكذا معادلات لجرانج لحركة الجسيمات الصلبة. كما اعتمد النموذج المقترح على ربط معادلات الاستمرار للغاز والجسيمات مستخدما نموذج اضطراب طاقة الحركة ومعادلة التشتت. كما يأخذ النموذج فى الاعتبار التأثير المتبادل لكل من الغاز والجسيمات كل منهما على الأخر وكذا اصطدام الجسيمات الصلبة مع أسطح هذه القنوات وارتدادها. وتهتم هذه الورقة بدراسة تأثير كل من سرعة الغاز الابتدائية ، نسبة تدفق الجسيمات إلى تدفق الغاز (معدل تحميل الجسيمات) ، نسبة الاتساع ، ارتفاع القناة عند المدخل وكذا قطر الجسيمات على كل من توزيعات السرعة فى اتجاه السريان والعمودية عليها لكل من الغاز والجسيمات الصلبة داخل القناة. وللتأكد من النموذج المقترح ودرجة الاعتماد عليه فقد أجريت مقارنة بين نتائج النموذج المقترح ونتائج نظرية وعملية سابقة منشورة لآخرين. وقد أظهرت هذه المقارنة توافقا مرضيا. كما أوضحت نتائج هذه الدراسة تأثير كل من سرعة الغاز الابتدائية ، معدل تحميل الجسيمات ، نسبة الاتساع ، ارتفاع القناة عند المدخل وكذا قطر الجسيمات على كل من توزيعات السرعة فى اتجاه السريان والعمودية عليها لكل من الغاز والجسيمات الصلبة داخل القناة وكذلك على مسار هذه الجسيمات داخل هذه القنوات وخصوصا فى منطقة السريان الدوامى للجسيمات صغيرة الحجم. كما أوضحت الدراسة أهمية النتائج التى تم الحصول عليها لاستخدامها فى فهم سلوك كل من الغاز المضطرب وحركة الجسيمات الصلبة خلال هذه القنوات.

Keywords: Turbulent flow, 2-D sudden expansion, Gas-solid two-phase, Two-way coupling, Particle collision, Particle trajectory

1. Introduction

Two-phase flows are commonly found in many engineering and natural processes such as, solid transport, coal fired power plants, food, chemical industries, pneumatic dryers and moving of dusty gas in heat exchanger. A better understanding of two-phase flow is important to improve performance or safety of the engineering systems as well as to reduce cost or pollutant emission. Therefore, solid particle separation and determination of particles trajectories are of great importance and it is necessary to predict the path of the particle, or the so-called particle trajectory. The combined effect from turbulence and other mechanisms such as Brownian diffusion, gravitational settling and electrostatic effects were studied by Ganic and Mastanaiah [1]. Complexity criteria in analyzing gas-particle flows arises when considering both the inertia of solid particles and the lift force on the particles due to a shear of the gas-phase flow [2]. The velocities of the particles can be, in general, different from the gas velocity and the particle streamlines may be deviated from those of the gas. This is consequently leads to distinct coupled momentum equations for the

two phases. Ebert [3] and Abou-Arab and Abou-Ellil [4] studied the interaction between the motion of particles and their turbulent carrier fluid flow. They reported that the turbulence occurs in the flow of the carrier fluid exerts a substantial influence on the motion of suspended particles. The motion of micron-sized aerosols in a turbulent gas flow was studied by Simo and Lienhard [5]. They reported that the inertial effects depend on the relative magnitude of the particle relaxation time. Martin and James [6] examined the motion of a small rigid sphere in a non-uniform flow. They determined separately the forces, which affect the small particle from the undisturbed flow and the disturbance flow created by the presence of the sphere. Some works were carried out [7-9] to determine the deposition velocities of spherical and nonspherical particles from gas flow in a horizontal pipe. It was observed that most of the previous researches show that the particles deposition, can be characterized by the intermediate values of the effective relaxation time and the particle shape or geometry. Founti et al. [10], investigated experimentally and numerically the effects of particle collisions on the characteristics of the particle motion in a vertical downward flowing sudden expansion flow. The results shown that the collisions between the particles induce small variation of the fluid – particle slip velocities and reduce the turbulent kinetic energy created from the dispersed phase. Also Founti et al. [11] extended their work, presented in [10], and studied the effects of increasing particle loading in an axisymmetric vertical, liquid–solid sudden expansion flow. They concluded that, increasing the particle concentration affected the local flow behavior, with most obvious consequences within the recirculation zone and near the wall region. Xi-Qing Chen [12] studied numerically the effect of using multi grid on the computations of turbulent particle-laden flows in a horizontal channel with sudden expansion. Zhang et al. [13-15] simulated numerically gas-particle sudden-expansion flows using an improved stochastic separated flow (ISSF). In their study the particle-particle interactions, the pressure gradients, the virtual mass, the effects of particle rotation, shear lift and Magnus lift due to particle rotation on the flow structure especially near the wall were not included. Comparison of three separated flow models was made by Zhang et al. [16]. In their work, comparison among the Improved Stochastic Separated Flow (ISSF) model and two widely used trajectory models (DSF and SSF) Deterministic Separated Flow (DSF) models and stochastic separated flow model respectively are made. They concluded that, ISSF model has distinct advantage over the other separated models while DSF model is capable of obtaining a solution with very few computational particles, but the particle turbulent dispersion is greatly underestimation. Mofreh [17] investigated numerically the flow behavior and particle trajectory in rectangular horizontal duct neglecting the effect of dispersed phase on the gas phase (mutual effects or one way coupling). Therefore, the present work continued the investigation given in [17] to study the effect of different size distribution of solid, mass loading ratio, channel geometry and initial flow velocity on the flow behaviour in a horizontal channel with sudden expansion. In addition the mutual effects between particulate phase and gas phase and also the effects of, gravity, particle rotation, shear lift and Magnus lift due to particle rotation, which were neglected in the previous studies are considered.

2. Basic equations

The fluid model based on Eulerian approach and the trajectory model based on the Lagrangian approach [12-20] are considered here. In addition the effect of flow parameters on the flow behavior in a horizontal channel with sudden expansion are studied numerically using modified k-ε model to simulate the gas-solid two-phase flow in ducts taking into account the effect of particle rotation, shear lift and Magnus lift due to particle rotation on the flow structure.

2.1. Basic equations of gas-phase flow

Sudden-expansion gas-solid two-phase flow as shown in fig. 1 is considered to be steady, two dimensional and turbulent. The

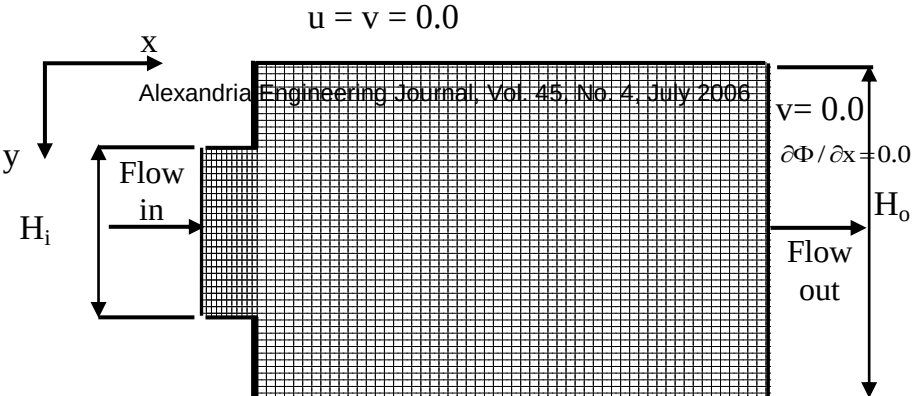

a- Duct geometry, inlet and boundary conditions and computational grid.

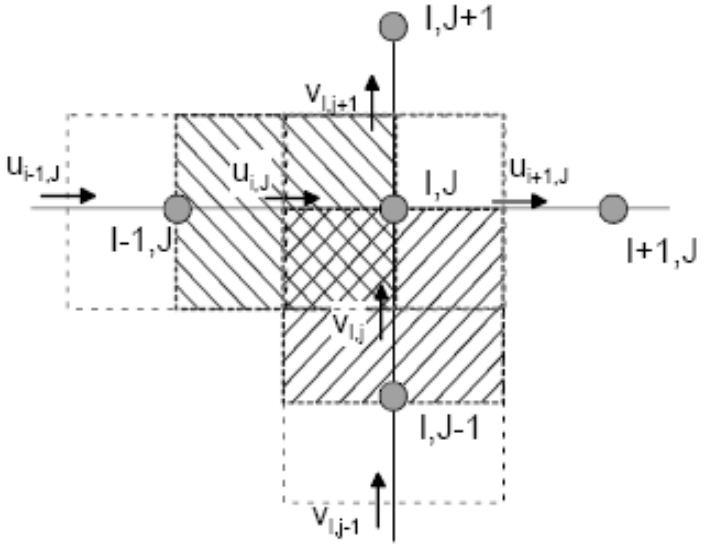

b- Computational cell

Fig. 1. Duct geometry, inlet and boundary conditions and computational cell.

general form of the Reynolds-averaged equations of continuous phase is expressed in cartesian coordinates as in [12-20] as follows,

$$\frac{\partial}{\partial x}(\alpha\rho u\Phi)+\frac{\partial}{\partial y}(\alpha\rho v\Phi)=\frac{\partial}{\partial x}\left(\alpha\Gamma_{\Phi}\frac{\partial\Phi}{\partial x}\right)+\frac{\partial}{\partial y}\left(\alpha\Gamma_{\Phi}\frac{\partial\Phi}{\partial y}\right)+S_{\Phi}-S_{p}^{\Phi} \quad (1)$$

Where, Φ is the generalized dependent variable (representing 1, u, v, k and ε for the conservation of mass, momentum in x and y directions, turbulence energy and its dissipation rate, respectively). Γ_{ϕ} is the transport coefficient, S^{Φ} is the source term of the continuous phase itself, and $S_p{}^{\Phi}$ is the source term due to gas-solid interaction. The meaning for each governing equation is given in table 1. The empirical constants used by many investigators [12-20] for the turbulence model are given in table 2.

Table 1
Governing equations of gas-phase

Conservation of	Φ	$\Gamma\Phi$	S^{Φ}	S_p^{Φ}
Continuity	1	0	0	0
X- momentum	u	μ_{eff}	$\frac{\partial(\alpha p)}{\partial x}+\frac{\partial}{\partial y}\left(\alpha\mu_t\left(\frac{\partial v}{\partial x}\right)\right)+\frac{\partial}{\partial x}\left(\alpha\mu_t\left(\frac{\partial u}{\partial x}\right)\right)$	$\frac{1}{V_c}\sum F_x$
Y-momentum	v	μ_{eff}	$-\frac{\partial(\alpha p)}{\partial y}+\frac{\partial}{\partial y}\left(\alpha\mu_t\frac{\partial v}{\partial y}\right)+\frac{\partial}{\partial x}\left(\alpha\mu_t\left(\frac{\partial u}{\partial y}\right)\right)$	$\frac{1}{V_c}\sum F_y$
Turbulent kinetic energy	k	$\frac{\mu_{eff}}{\sigma_k}$	α (G-$\rho\varepsilon$)	S_p^k
Energy dissipation	ε	$\frac{\mu_{eff}}{\sigma\varepsilon}$	$\alpha\frac{\varepsilon}{k}$ (C_1 G-C_2 $\rho\varepsilon$ -R)	S_p^{ε}

Table 2
Values of model constants

Model constants	C_1	C_2	C_μ	σ_k	σ_ε	S_P^K	S_P^ε
	1.44	1.92	0.09	1.0	1.3	eq. (6)	eq. (7)

Where, the turbulent kinetic energy generation term G, is defined as,

$$G=\mu_t\left(2\left(\frac{\partial u}{\partial x}\right)^2+2\left(\frac{\partial v}{\partial y}\right)^2+\left(\frac{\partial v}{\partial x}+\frac{\partial u}{\partial y}\right)^2\right)$$

$$\mu_{eff}=\mu\left[1+\sqrt{\frac{C_\mu\rho}{\mu}}\frac{k}{\sqrt{\varepsilon}}\right]^2,\ \mu_t=\mu_{eff}-\mu\ . \qquad (2)$$

The rate of strain R in the ε equation of k- ε model is expressed as given in [19] by,

$$R=\frac{C_\mu\eta^3((1-\eta/\eta_o)}{1+\chi\eta^3}\varepsilon$$

where, χ = 0.015

$$\eta=S\frac{k}{\varepsilon},\qquad S=\sqrt{G/\mu_t}$$

The effect of particulate phase on the turbulence structure can be formulated as reported in refs. [15, 19] for k and ε equations respectively as follow,

$$S_P^k=2.k\left[\frac{\rho_p}{\tau_p}\right]\left[1-\exp\left(-B_k\frac{\tau_P}{\tau_l}\right)\right]. \qquad (3)$$

$$S_P^k=2.\varepsilon\left[\frac{\rho_p}{\tau_p}\right]\left[1-\exp\left(-B_\varepsilon\frac{\tau_P}{\tau_l}\right)\right]. \qquad (4)$$

Where B_k, B_ε are constants and taken as 0.09 and 0.4 respectively as in [19]. While, $\tau_l = k/\varepsilon$ and τ_P is the particle relaxation time.

2.2. Basic equations of particle-phase flow

Particles are assumed to be non-deformable and spherical. The ratio of particle density and the fluid density (ρ_p/ρ_f) is approximately 2×10^3. Virtual mass force and pressure gradient force are of the order of (ρ_f/ρ_p), as concluded by other investigators; hence these forces are neglected in the present study. In these simulations particle-particle interactions is also neglected. The solid phase is treated by the Lagrangian approach, a few thousands of computational particles 'parcels' were traced through the flow field in each coupling iteration. After each time step the new position of the parcels and the new translational and angular velocities are calculated from the equations of motion as in [11, 21-22] through,

$$\frac{d\vec{X}_p}{dt} = \vec{U}_p, \tag{5}$$

$$m_p \frac{d\vec{U}_p}{dt} = \sum \vec{F}, \tag{6}$$

where, $\sum \vec{F} = \vec{F}_D + \vec{F}_{SL} + \vec{F}_{LM} + \vec{F}_G$

$$I_P \frac{d\vec{\omega}_p}{dt} = \vec{T}$$

$$\vec{T} = \pi \mu D_p^3 \left[\frac{1}{2}\nabla \times \vec{U} - \vec{\omega}_p\right], \tag{7}$$

where, $\vec{X}_p$ is the particle position vector, $\vec{U}, \vec{U}_p$ are the gas and particle velocity vectors, $\vec{\omega}_p$ is the particle angular velocity vector, T is the torque acting on a rotating particle due to the viscous interaction with the fluid flow, I_p is moment of inertia and m_p is the particle mass, $\vec{F}_D, \vec{F}_{SL}, \vec{F}_{LM}$ and F_G are the components of the force arising from drag, shear lift Magnus lift due to particle rotation and gravity respectively and calculated as depicted in [11, 22-23] respectively as follows,

The drag force is calculated from:

$$F_D = \frac{3}{4} \frac{\rho\ m_p}{\rho_p\ D_p} C_D (\vec{U} - \vec{U}_p)\left|\vec{U} - \vec{U}_p\right|. \tag{8}$$

The relationship between the drag coefficient; C_D, and Reynolds number; Re_P, can be expressed using the empirical formulas as in [17, 23];

$$C_D \begin{cases} 24/Re & Re \le 1 \\ 24/\mathrm{Re}^{0.646} & 1 < Re \le 400 \\ 0.5 & 400 < Re \le 3x10^5 \\ 0.000366\,Re^{0.4275} & 3x10^5 < Re \le 2\times10^6 \\ 0.18 & Re > 2\times10^6 \end{cases}. \tag{9}$$

where, $Re_p = \rho D_p \left|\vec{U} - \vec{U}_p\right| / \mu$ is the particle Reynolds number.

The shear lift force due to the non-uniform relative velocity over the particle is expressed as reported in refs. [11, 23] as,

$$\vec{F}_{SL} = 1.615 . D_p \mu \mathrm{Re}_s^{0.5} C_{SL} \left[\left(\vec{U} - \vec{U}_p\right) \times \vec{\omega}_f\right]. \tag{10}$$

where, $\vec{\omega}_f = 0.5(\nabla \times \vec{U})$ is the fluid rotation, $Re_s = \rho D_p^2 \left|\vec{\omega}_f\right| / \mu$ is the particle Reynolds number of the shear flow and the coefficient C_{SL} is given as in [23] by,

$$\begin{aligned} C_{SL} &= (1\text{-}0.3314\gamma^{0.5}) e^{-Re_p/10} + 0.3314\ \gamma^{0.5} \quad Re_p \le 400 \\ &= 0.0524\ (\gamma\, Re_p)^{0.5} \qquad Re_p > 400. \end{aligned} \tag{11}$$

where γ is the correction function proposed by [23] and is defined by the ratio between R_{es} and Re_p as,

$$\gamma = \frac{\mathrm{Re}_s}{0.5\,\mathrm{Re}_p}. \tag{12}$$

The Magnus lift due to particle rotation is expressed as in [11, 24] by,

$$\vec{F}_{LM} = \frac{1}{2}\rho \vec{V}_r^2 \frac{\pi D_p^2}{4} C_{LM} \frac{\vec{\omega}_r \times \vec{V}_r}{|\vec{\omega}_r||\vec{V}_r|} \quad . \tag{13}$$

where the quantities $\vec{V}_r = \vec{U} - \vec{U}_p$ and $\vec{\omega}_r = \vec{\omega}_f - \vec{\omega}_p$ are the instantaneous relative linear and angular velocities between local fluid and the particle, respectively. The Magnus lift coefficient may be expressed as in [22] by,

$$C_{LM} = \frac{D_p|\vec{\omega}_r|}{|\vec{V}_r|} \qquad Re_p \le 1$$

$$= \frac{D_p|\vec{\omega}_r|}{|\vec{V}_r|}(0.178 + 0.822\,\mathrm{Re_p}^{-0.522}) \qquad 1 < Re_p < 100 \tag{14}$$

Finally the gravitational force is,

$$\vec{F}_G = m_p \vec{g}\left(\frac{\rho_f}{\rho_p} - 1\right). \tag{15}$$

2.3. Inlet and boundary conditions

The above differential equations, eqs. (1 and 8-10) are coupled with the definitions and complementary equations to compute the gas and particle velocities and particle trajectories under the initial and boundary conditions for gas and particulate phases.

2.4. Initial and boundary conditions

At the inlet, the streamwise velocity profile for gas phase (air) is assumed fully developed turbulent velocity profile in a straight channel connected upstream the sudden expansion, where the transverse velocity is assumed to be zero. The inlet particle velocity is taken approximately equal gas inlet velocity. At outlet, the gradient of flow variables in the flow direction; $\partial\Phi/\partial x = 0$ (Neumann conditions), and the transverse velocity v which is set to zero. At the solid wall boundaries, however, $u = v = 0.0$, no-slip conditions.

Because the k and ε equations are not solved at the grid point adjacent to the wall, a modeling scheme is required to simulate the variation of eddy viscosity, μ_t. For this purpose the mixing length approach is adopted where the eddy viscosity is modeled as a function of mixing length as in ref. [25] by,

$$\mu_t = \rho.\ell_m^2\left[2\left(\frac{\partial u}{\partial x}\right)^2 + 2\left(\frac{\partial v}{\partial y}\right)^2 + \left(\frac{\partial v}{\partial x} + \frac{\partial u}{\partial y}\right)^2\right]^{1/2}. \tag{16}$$

where, ℓ_m is the mixing length and is calculated for smooth walls, from Van Dsiert`s equation, [25] as,

$$\ell_m = Ky_p\,(1 - exp\,(-y^+ / A)). \tag{17}$$

Where, A is constant and takes the value of 26 for smooth walls in the equilibrium near wall layer. Also to improve the accuracy of k-ε the second-order finite difference formula is used to evaluate the velocity gradient at the wall as, [26].

$$\left(\frac{\partial u}{\partial y}\right)_w = \frac{-8u_w + 9u_1 - u_2}{3y_w} + O(y_w^2). \tag{18}$$

Where, y_w is the thickness of the cell adjacent to the wall, $u_w = 0.0$ for stationary wall and no slip condition, u_1 and u_2 are the velocities at the next two grid points respectively.

2.5. Particle wall interaction

As reported in ref. [27] the model of particle wall adhesion is based on energy balance around the particle wall collision, additionally, in the present study electrostatic part was neglected, so the involved energy balance becomes,

$$E_{k_{in}.1} = E_{vdW} + E_{k_{in}.2} + E_1. \tag{19}$$

Where $(E_{k_{in}.1}, E_{k_{in}.2})$ is the kinetic energy before and after the wall collision, (E_{vdW}) is the energy ratio describing the adhesion with Van der Waals and (E_1) is the energy loss of a particle due to wall collision which is defined as,

$$E_1 = E_{k_{in}.1}\left(1 - e^2\right). \quad (20)$$

The prerequisite of adhesion is that the particle is not able to leave the wall after the wall collision, i.e., $\left(E_{k_{in}.2} = 0.0\right)$. Inserting this condition with eq. (20) in eq. (19) yields a critical particle velocity.

$$w_{p.cr} = \frac{\hbar\varpi}{eD_p 4\pi^2 Z_0^2}\sqrt{\frac{3}{4H\rho_p}}. \quad (21)$$

The critical velocity depends on the Liffschitz-van der Waals constant, $\hbar\varpi$ (4×10^{-19}), as reported in [27], the material of the pipe wall and the particle, the particle diameter D_p, the distance at contact z_o(4×10^{-10}), the strength of the pipe wall H(250×10^6 N/m^2).

The condition of rebound is achieved if the particle velocity before collision, w_{p1} greater than the critical particle velocity, $w_{p,cr}$. The solution of the momentum equations with Coulombs law of friction yields a set of equations for non-sliding and sliding collision process [24, 29]. This model was used and verified by [28]. The non-sliding collision takes place when the following condition is valid,

$$\left|u_{p1} - \frac{D_p}{2}\vec{\omega}_{p1}\right| \le \frac{7}{2}\mu_0(1+e)v_{p1} \quad . \quad (22)$$

Here, the subscript 1 refers to the particle velocity components before collision, μ_o is the static coefficient of friction. Furthermore the velocity components before impact and after rebound are calculated for a collision without sliding as follows,

$$u_{p2} = \frac{1}{7}(5u_{p1} + D_p\vec{\omega}_{p1}). \quad (23)$$

$$V_{p2} = -\, e\, v_{p1}. \quad (24)$$

$$\omega_{p2} = 2\frac{u_{p2}}{D_p}. \quad (25)$$

While, for the so-called sliding collision the change of translational and rotational velocities are calculated as,

$$U_{p2} = u_{p1} - \mu_d \ (1+ e)\ \varepsilon_o\, v_{p1}. \quad (26)$$

$$V_{p2} = -\, e v_{p1}. \quad (27)$$

$$\omega_{p2} = \omega_{p1} + 5.0\mu_d(1+e)\varepsilon_0\frac{V_{p1}}{D_p}. \quad (28)$$

In these equations, μ_d is the dynamic friction coefficient, and ε_o determine the direction of the motion of the particle surface with respect to the wall which is given as in [24, 29] by,

$$\varepsilon_o = sign\left(u_{p1} - \frac{D_p}{2}\omega_{p1}\right). \quad (29)$$

The values of coefficient of restitution, e static and dynamic coefficients of friction, μ_o and μ_d are taken as 0.9, 0.4 and 0.15 respectively as in [29] for all calculations.

2.6. Numerical procedure and convergence

The resulting system of equations has been solved used a finite differencing descretisation scheme based on a staggered grid arrangement shown in fig. 2. Pressure-velocity coupling was realised by SIMPLE algorithm [26, 30]. The solution procedure for the fluid and particulate phase is as follow:

1. A converged solution of gas phase is calculated without source term of the dispersed phase and with gas void fraction, α of unity. Conversion solution is accepted at normalized residuals less than 0.002.
2. By numerically integrating the translational and rotational equation of motion for each parcel in a small time step Δt which is firstly assumed by ($0.33.D_P/u_p$) using fourth order Runge-Kutta method, a large number of discrete parcels are traced through the flow field. The time step is selected to achieve trajectory independent for each run case.
3. The void fraction for dispersed phase, β and for gas phase, α are calculated using trajectory method as [31],

$$\beta = \sum_{traj}\frac{n_k\Delta t_k V_p}{V_c}, \quad \alpha = 1-\beta. \quad (30)$$

Here, n_k is the number of actual particles in the computational particle 'parcel', k , V_P is the volume of the particle, V_c is the volume of computational cell and $\sum_{traj}$ means summing over all trajectory passing through the computational cell. The source term of dispersed phase in the gas momentum equation is calculated as in [22] by,

$$S_p = \frac{\beta \rho_p}{m_p n} \sum_{k=1}^{n} (\vec{F}), \tag{31}$$

where, n is the number of trajectories passing through the computational cell.

4. The gas flow field is recalculated taking into account the source term and void fractions resulting in step 3

5. Repeat step 2 through 4 until the maximum error in the streamwise gas velocity between two successive coupled iteration is less than 0.0001 of the inlet mean velocity. Convergence history of mean streamwise flow velocity (normalized error) for the case of comparison is shown in fig. 3.

2.7. Model validation

A test for the present model is carried out for a typical case of sudden-expansion particle laden flow, which has a recirculating region and widely found in engineering. So the models has been tested and validated against the numerical results of [14] and experimental results of Summerfeld [32]. The test case is carried out with the geometry of the circular test section and flow parameters similar to those in [14, 32] and summarized in table-3. The comparison illustrated in fig. 3, shows a good agreement for both axial mean velocity and turbulent kinetic energy profiles. The difference between the published data and some data of the present predictions may be a result of two factors. One due to the ability of the k-ε model for liquid phase in sudden expansion flow. The other is a result of the assumed inlet conditions, as no experimental data available.

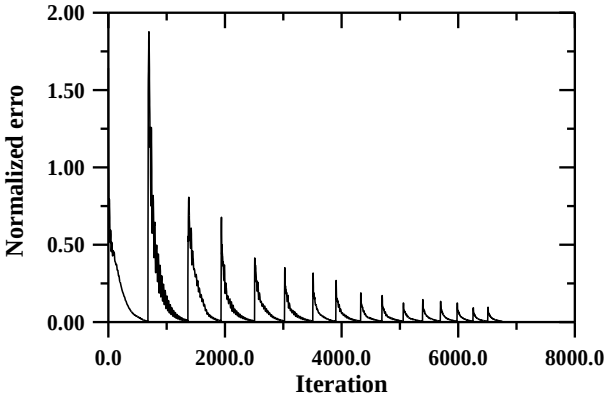

Fig. 2. Convergence history of streamwise flow velocity, (normalized error).

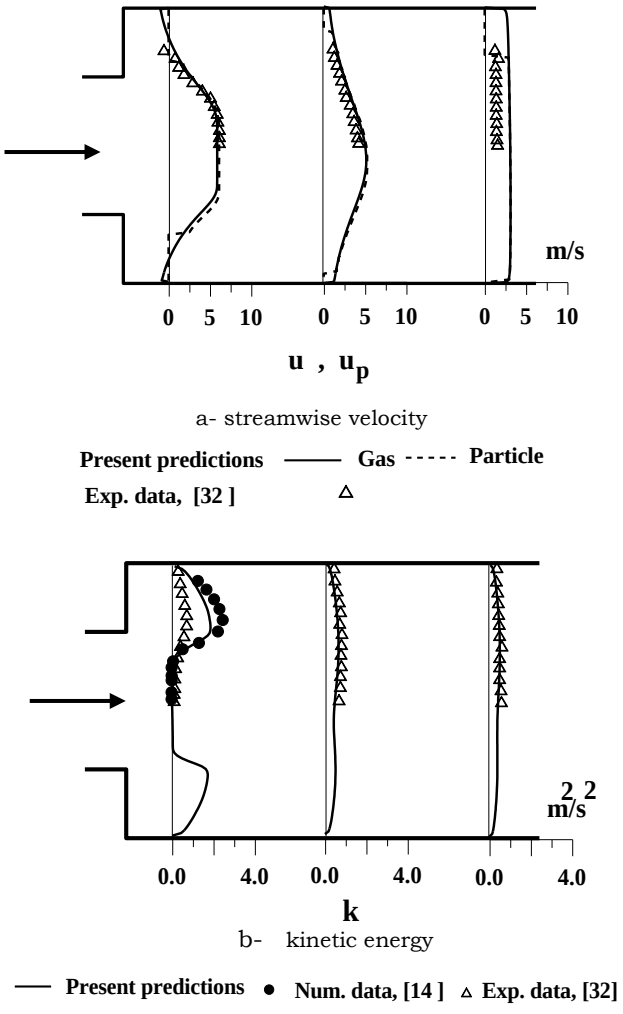

Fig. 3. Comparison between present results and the previously published data of [14, 32].

Table 3
Flow parameters of comparison test case

Property	Liquid-phase	Particle-phase
Density, ρ	830 kg/m^3	2500 kg/m^3
Kinetic viscosity	5.205 cS	-
Inlet velocity	6.021 m/s	6.021 m/s
Mass flux,	2.29 kg/s	0.213 kg/s

4. Results and discussion

A two-phase gas-solid flow through a two-dimensional sudden expansion of a channel has length of 1 m is used for all calculations. The flow characteristics through the channel are studied for different height ratio (HR), inlet height (H_i), particle diameters (D_p), mean air inlet velocity (U_o), and mass loading ratio. In addition the effect of these parameters on particles trajectories are presented. All the particles have been introduced in the flow with approximately the same fluid bulk velocity. The particulate phase consists of spherical particles with diameter varied from 20 to 400 μm, with a density of 2600 kg/m^3, and the mass loading ratio for the mixture was varied from 0.1 to 1.5 which was assumed to be uniformly distributed. About 10000 particles per parcel are introduced.

4.1. Velocity profiles

The velocity profiles for gas and solid phases of a two-phase flow through a horizontal channel with sudden-expansion are investigated for different inlet flow velocity ranged from 1 to15 m/s, channel height ratio HR, was ranged from 1.25 to 1.75 at constant inlet height 0.0125 m. The channel inlet height, H_i was varied from 0.00625 to 0.025 m at constant height ratio of 2. The velocity profiles of gas and solid (u , v) respectively for different inlet flow velocity, are shown in figs. 4 and 5. The streamwise gas velocity profiles show the presence of recirculation flow regimes where, the streamwise velocity drops from positive value at the center to negative value near the wall. Generally the streamwise

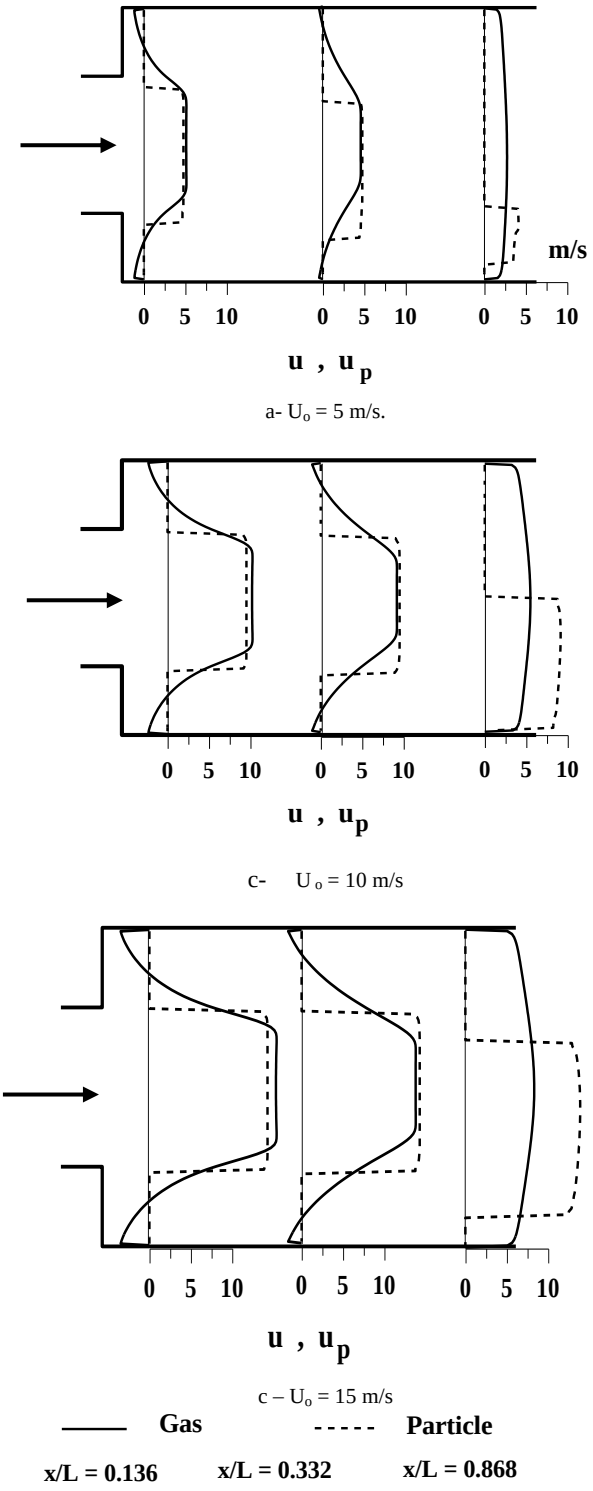

(D_p = 400 μm , m_R = 0.1, HR = 2).

Fig. 4. Effect of inlet gas velocity on streamwise velocity profiles for gas and particulate phases.

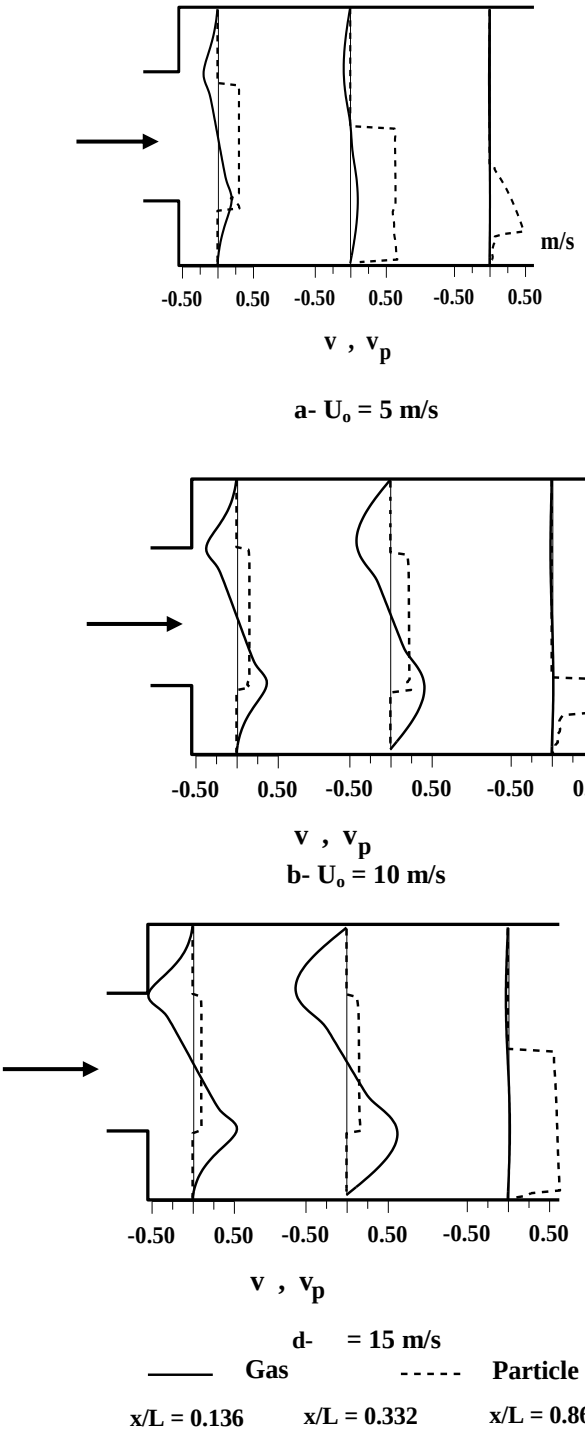

Fig. 5. Effect of inlet gas velocity on transverse velocity profiles for gas and particulate phases.

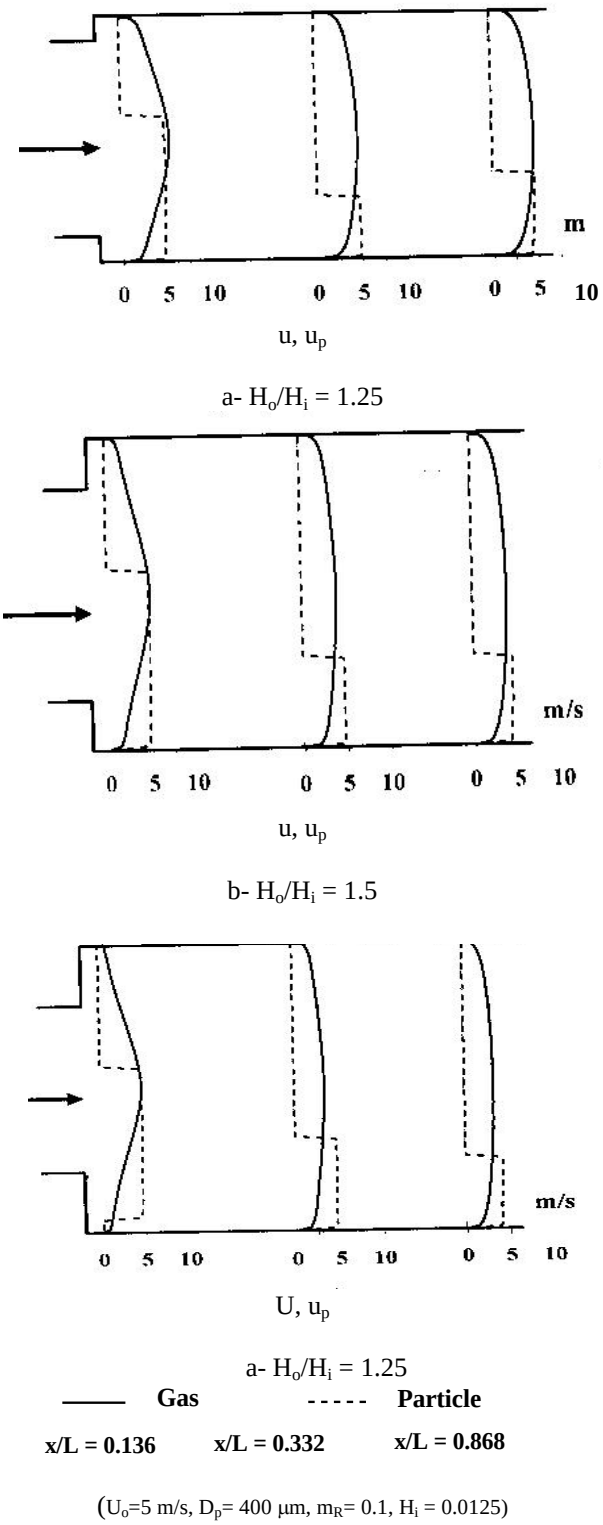

Fig. 6. Effect of height ratio on sreamwise velocity profiles for gas and particulate phases at constant inlet height.

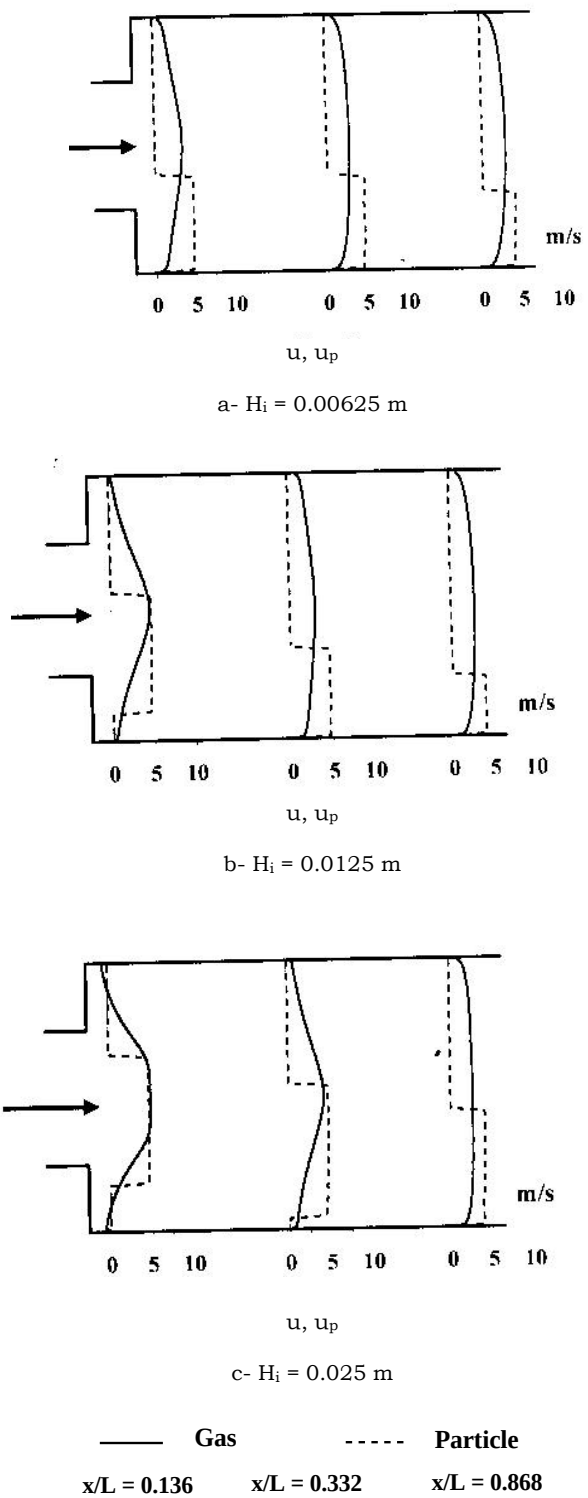

Fig. 7. Effect of inlet height on streamwise velocity profiles for gas and particulate phases at constant height ratio.

gas velocity profile through the channel in x-direction becomes more uniform as the duct length increases. Whilst the velocity component (v), in the y-direction decreases with increasing the channel length and approaches to become zero.

Figs. 6-7 show the effects of height ratio and inlet height on gas and particle streamwise velocities. Predicted streamwise velocity profiles for both gas phase and particle phase for channel with sudden expansion have three different height ratio of (H_o/H_i = 1.25, 1.50 and 1.75) is shown in fig. 6. The figure illustrates that, the particle velocity first lags behind the gas phase velocity and then exceeds it. In the reverse flow region a higher velocity slip between two phases is obtained as the height ratio of the channel increases. Fig. 7 shows the predicted velocity profiles for both gas phase and particle phase for channel with sudden expansion with constant height ratio of 2 but have three different values of inlet height (H_i = 0.00625, 0.0125 and 0.025 m) respectively. The figures indicate that, in the reverse flow region slip velocity close to the wall appear to be increase between two phases as the inlet height of the channel decreases. This can be attributed to a relative of increase of the number of particle wall collisions.

The effect of particle diameter on the particle velocity profiles is presented in fig. 8-a and b. The figure indicates that the heavy particles have greater values of both streamwise and transverse velocities. While fig. 8-c shows the effect of particle diameter on the variations of the turbulent kinetic energy of gas phase along the channel axis. The figure indicates that there are two maximum values of turbulent kinetic energy in the upstream, further progress along the channel axis the maximum value moves to the axis in the down stream.

4.2. Particle trajectory

Figs. 9-13 show the effects of loading ratio, inlet flow velocity, particle diameter, height ratio and inlet height on particle trajectories. fig. 9 shows the particles trajectories for different mass loading ratio. The figure reveals that the solid particles are more dispersed

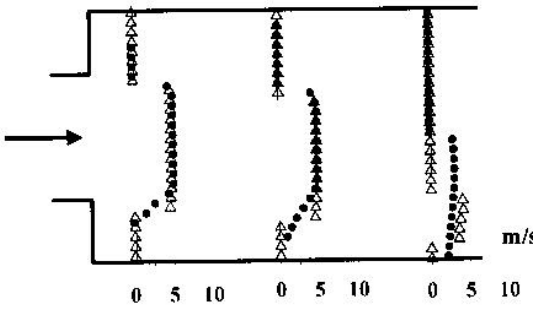

u_p

a- streamwise particle velocity

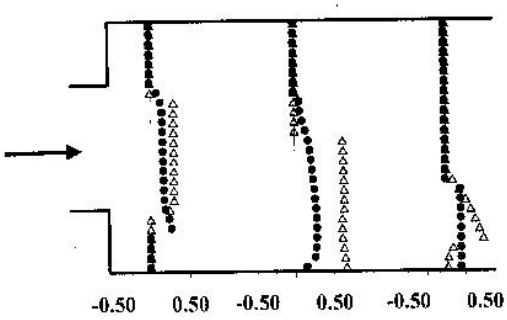

v_p

b- streamwise particle velocity

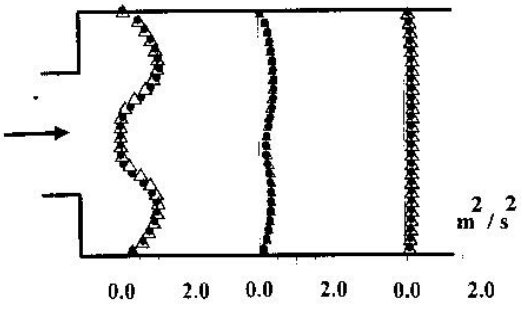

k

c- gas turbulent kinetic energy

• **Dp = 50 m** △ **Dp = 400 m**

x/L = 0.136 **x/L = 0.332** **x/L = 0.868**

(U_o= 5 m/s , m_R= 0.1, HR =2)

Fig. 8. Effect of particle diameter on particle velocity profiles and turbulent kinetic energy.

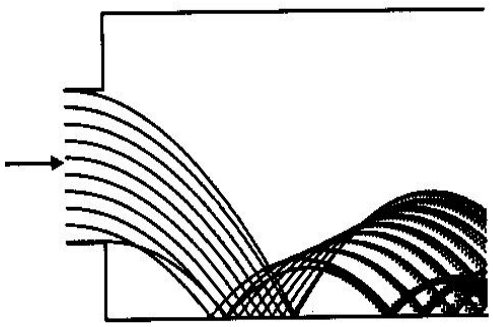

a- m_R = 0.5

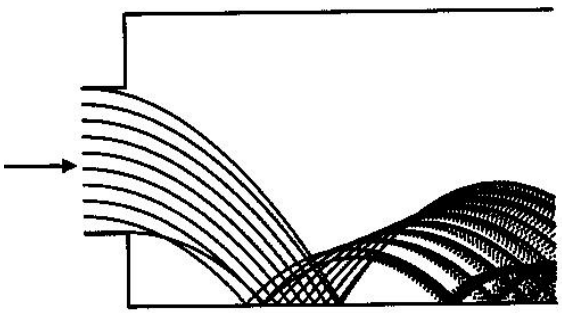

b- m_R = 1.0

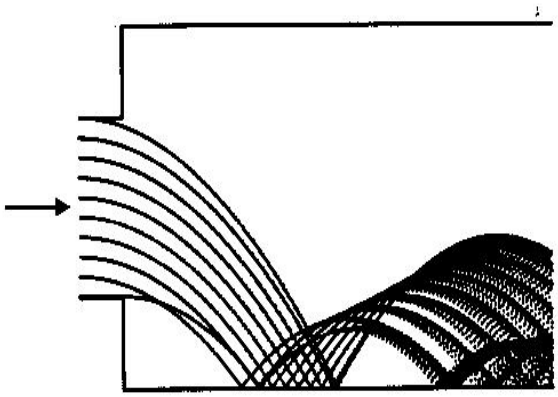

c- m_R = 1.5

(U_o= 5 m/s , D_p = 400 μm, HR =2)

Fig. 9. Effect of mass loading ratio, m_R on particle trajectory.

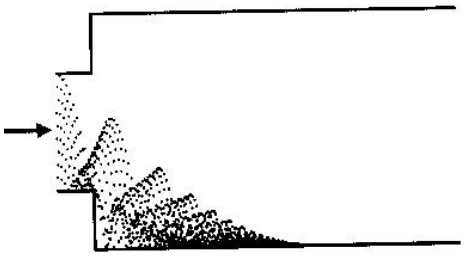

a- U_o = 1 m/ s

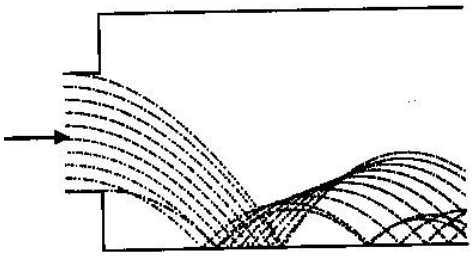

b- U_o = 5 m/ s

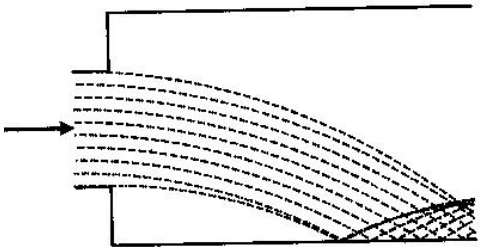

c- U_o = 10 m/ s

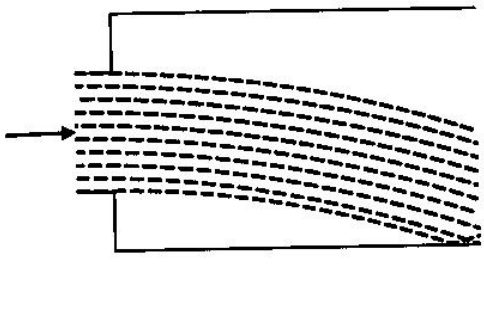

d- U_o = 15 m/ s

(D_p = 400 μm , m_R = 0.1, HR = 2)

Fig. 10. Effect of inlet gas velocity on particles trajectories.

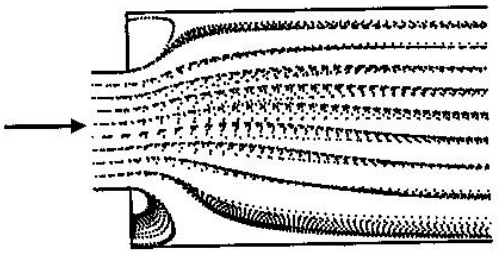

a- D_p = 10 μm

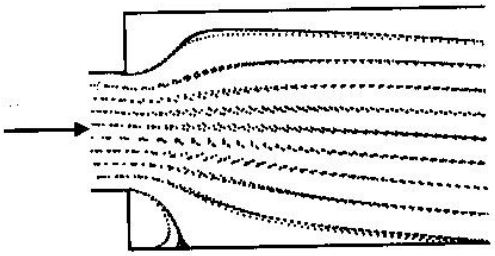

b- D_p = 20 μm

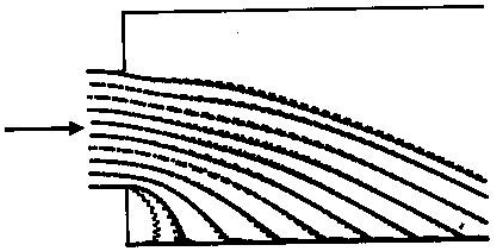

c- D_p = 50 μm

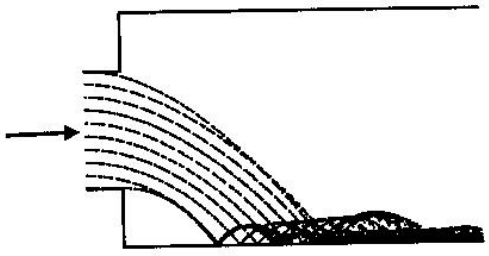

d- D_p = 150 μm

(U_o= 5 m/s, m_R = 0.1, HR = 2)

Fig. 11. Effect of particle diameter on particles trajectories.

with increasing mass loading ratio. From velocity profiles previously shown in figs. 4-7 it can be seen that, although all particles entered under the same conditions, during their traveling they acquired different velocities and dispersed in the flow and the particles don't follow the fluid. If a particle moves faster than the fluid by $u_{slip} = |u| - |u_p|$, the time of interaction with the large eddies

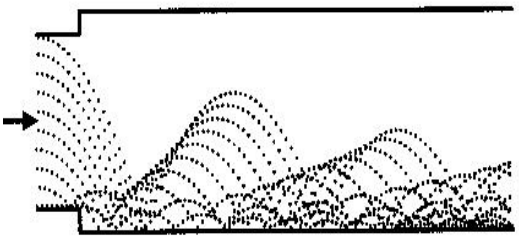

a- H_o/H_i = 1.25

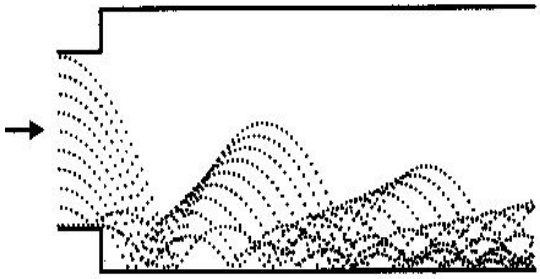

b- H_o/H_i = 1.5

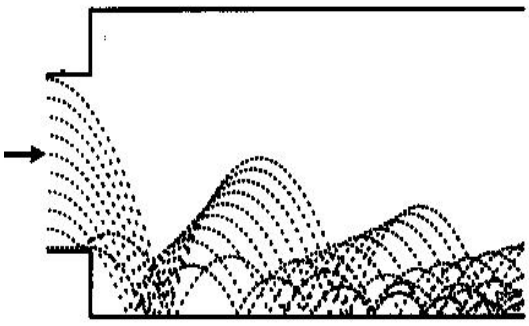

c- H_o/H_i = 1.75

(U_o=5 m/s, D_p= 400 μm, m_R=0.1, H_i =0.0125)

Fig. 12. Effect of height ratio on particle trajectories.

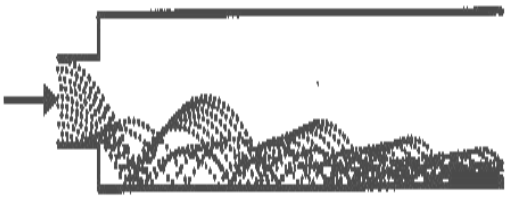

a- H_i = 0.00625 m

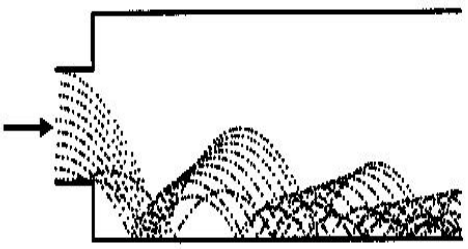

b- H_i = 0.0125 m

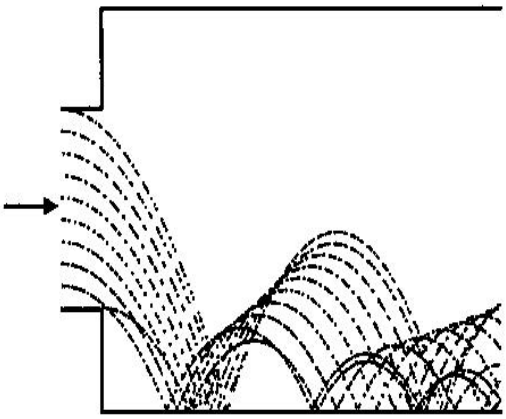

c- H_i = 0.025 m

(U_o= 5 m/s, D_p = 400 μm, m_R = 0.1, HR = 2)

Fig. 13. Effect of inlet height on particle trajectories.

and particle dispersion are reduced. It can be anticipated that for the particles to enter the recirculation zone as shown in fig. 10 by crossing the shear layer, the Stockes number, $St = (\tau_v / \tau_F)$ for the shear layer and for the recirculation zone should be less than unity then the particles are expected to respond to fluid. It is also clear from fig. 10 that the

initial momentum affects the particle trajectory.

Changes in particles trajectory and particle velocity profiles through the tested duct at different values of particle diameter D_p, height ratio and inlet height, at constant mean inlet gas velocity are illustrated in figs. 11-13. From these figures generally it can be noticed that, the required duct length for the solid particles to collision with bottom duct surface, x_c, decreases with decreasing the initial particle location(x_o, y_o). Fig. 11 declares that increasing the particle mean diameter, decreases the required duct length to ensure adequate particles collision. Also fig. 11 shows that at constant initial momentum the recirculation zone affects small particles, more than the heavy particles and the dispersion for heavy particles is higher than for small particles. The particles located near the wall move very slowly but due to the initial momentum, heavy particles accelerate where as the small particles start spinning and move very slowly in the positive direction. Particles can enter the recirculation zone, due to their history, with higher local mean velocities than the carrier gas depending on the size of the energy carrying eddy that drives the particle into the recirculation zone. In particular, close to the channel wall the carrier gas velocity is relatively small thus transferring momentum to the carrier gas is obtained. It is also noticed that, by decreasing particles diameter (small particles) the wall effect on the particle trajectory diminishes. For small particles it is also seen that the particles suspended with gas stream near the wall while in the core region the particles flow in approximately straight line. This may be due to that the viscous effect which exceeds the gravity effect.

5. Conclusions

The main conclusions drawn from this study are:

- The present model can estimate the particle trajectory, particle velocity as well taking into account the mutual effects of solid-phase on gas-phase.
- The flow velocity, location of particle in the channel and its size play an important role in the particle trajectory.
- The particles collision on the bottom surface of a two-dimensional straight channel occurs faster for lower initial particle location in the y-direction, large particles and slower flow velocities.
- The trajectories are influenced by the size of the particles, mass loading ratio and the locations of particles.
- The dispersion of heavy particles is higher than that for small particles.

Nomenclature

F is the force, N
G is the gravity acceleration, m.s^{-2}
H_i is the duct inlet height, m
H_o is the duct outlet height, m
HR is the height ratio (H_o / H_i)
L is the channel length, m
e is the restitution coefficient
m'_g is the mass rate of gas phase, kg.s^{-1}
m'_p is the mass rate of particulate phase, kg.s^{-1}
m_R is the mass loading ratio, (m'_p / m'_g)
P is the pressure, N.m^{-2}
t is the time, sec
u, v is the streamwise and transverse velocity components of the gas phase, m.s^{-1}
u_{p1}, v_{p1} is the streamwise and transverse particle velocities before collision, m.s^{-1}
u_{p2}, v_{p2} is the streamwise and transverse particle velocities after rebound, m.s^{-1}
U_o is the mean-bulk longitudinal velocity, m.s^{-1}
y is the normal coordinate measured from the upper wall, m, and
x is the axial coordinates along the axis of the duct, m.

Geek symbols

α is the gas phase void fraction,
β is the solid phase void fraction,
Φ is the general dependent variable,
$\omega_{p,i}$ is the particle angular velocity before impact and after rebound, rad.s^{-1}
ω_r is the relative angular velocity vector, rad.s^{-1}
μ is the laminar viscosity; N.s.m^{-2}

μ_t is the turbulent viscosity; $N.s.m^{-2}$
ν is the kinematic viscosity; $m^2.s^{-1}$
ρ is the gas density; $kg.m^{-3}$
τ_F is the time characteristic of the flow field, s and,
τ_V is the velocity or momentum response time s.

Subscripts

C	collision
D	drag
f	fluid
i	inlet section
LM	Magnus lift
o	outer section
p	particle
s	solid
SL	shear lift

References

[1] E.N. Ganic and K. Mastanaiah, "Investigation of Droplet Deposition from a Turbulent Gas Stream", Int. J. Multiphase Flow, Vol. 7, pp. 401-422 (1981).

[2] I. Ryuji, "Motion of Small Particles in a Gas Flow", J. Phys. Fluids, Vol. 27, pp. 33-41 (1984).

[3] F. Ebert, "Interaction between the Motion of Particles and Their Turbulent Carrier Fluid Flow", J. Particle and Particle Systems Characterization, Vol. 9, pp. 116-124 (1992).

[4] T.W. Abou-Arab and M. Abou-Ellail, "Modulation of Heat Transfer in Dusty Gas Pipe Flow ", Proceedings of 6 th Int. Conf. For Mech. Power Engng., Vol. 2, (II.1), Menoufia Univ., Cairo, Egypt, Sept. (1986).

[5] J.A. Simo, and J.H. Lienhard, "Turbulent Transport of Inertial Aerosols ", Proc. of National Heat Transfer Conference, Minneapolis, MN, USA, July 28 -31 (1991).

[6] R.M. Martin and J.R. James, "Equation of Motion for a Small Rigid Sphere in a Non-Uniform Flow ", J. Phys. Fluids, Vol. 26, pp. 883-889 (1983).

[7] E.E. Michaelides, "A Model for the Flow of Solid Particles in Gases ", Int. J. Multiphase Flow, Vol. 10 (1), pp. 61-77 (1984).

[8] M. Shapiro and M. Goldenbere, "Deposition of Glass Fibre Particles from Turbulent Air Flow in a Pipe ", J. Aerosol Science, Vol. 24, pp. 65-87 (1993).

[9] Y.P. Gorkov and E.E. Densiov, "Mathematical Modeling of Particle Deposition on Duct Walls", Thermal Engineering, Vol. 40 (1), pp. 60-62 (1993).

[10] M. Founti, Th. Achimastos and A. Klipfel, "Effects of Increasing Particle Loading in an Axisymmetric, Vertical, Liquid-Solid Sudden Expansion Flow ", Trans. Of ASME, Experimental and Computational Aspects of Validation of Multiphase Flow, CFD Codes, Fluids Eng. Div. Summer Meeting, Nevada, USA, FED-Vol. 180 (1994).

[11] M. Founti and A. Klipfel, "Experimental and Computational Investigations of Nearly Dense Two-Phase Sudden Expansion Flows", Experimental Thermal and Fluid Science, Vol. 17, issue 1-2, pp. 27-36 (1998).

[12] X.Q. Chen, "Multigrid Acceleration of Computations of Turbulent Particle-Laden Flows", Numerical Heat transfer, Part B, 40: pp. 139-162 (2001).

[13] H.Q. Zhang, C.K. Chan and K.S. Lau, "An Improved Stochastic Separated Flow Model for Turbulent Two-phase Flow ", Computational Mechanics Vol. 24, pp. 491-502 (2000).

[14] H.Q. Zhang, C.K. Chan and K.S. Lau, "Numerical Simulation of Sudden-expansion Particle-laden Flows Using an Improved Stochastic Separated Flow Model", Numerical Heat transfer, Part A, 40: pp. 89-102 (2001).

[15] H.Q. Zhang, C.K. Chan and K.S. Lau, "Numerical Simulation of Gas-particle Flows behind a Backward-Facing Step Using an Improved Stochastic Separated Flow Model ", Computational Mechanics Vol. 27, pp. 412-417 (2001).

[16] H. Zhang, C.K. Chan and K.S. Lau, "Comparison of Three Separated Flow Models ", Computational Mechanics Vol. 28, pp. 469-478 (2002).

[17] H.H. Mofreh, "Gas Particle Two-Phase Turbulent Flow in a Horizontal Sudden Expansion Channel ", Int., Mech. Eng. Conference and Expo, Kuwait 5-8 December (2004).

[18] E.E. Khalil, D.P. Spalding and J.H. Whitelaw, "The Calculation of Local Flow Properties in Two-Dimensional Furnace ", Int., Journal Heat Mass Transfer, Vol. 18, pp. 775-791 (1975).

[19] A. Eghlimi, A. Kouzoubov and C.A.J. Fletcher, "A New RNG-based Two-Equation Model for Predicting Turbulent Gas-Particle Flows", Int. Conf. on CFD in mineral and Metal Processing and Power Generation (1997).

[20] L.X. Zhou, W.Y. Lin and C.M. Liao, "Simulation of Particle-Fluid Turbulence Interaction in Sudden-Expansion Flows ", Powder Tech., Vol. 90, pp. 29-38 (1997).

[21] N. Huber and M. Sommerfeld, "Modeling and Numerical Calculation of Dilute-Phase Pneumatic Conveying in Pipe Systems ", Powder Tech., Vol. 99, pp. 90-101 (1998).

[22] C.K.K. Lun, and H.S. Liu, "Numerical Simulation of Dilute Turbulent Gas-Solid Flows in Horizontal Channels ", Int. J. Multiphase Flow, Vol. 23, pp. 575-605 (1997).

[23] R. Mei, "An Approximate Expression For The Shear Lift Force on a Spherical Particle at Finite Reynolds Number", Int. J. Multiphase flow, Vol. 18, pp. 145-147 (1992).

[24] M. Sommerfeld, " Modeling of Particle-Wall Collisions in Confined Gas-Particle Flows", Int. J. Multiphase flow, Vol. 183, pp. 905-926 (1992).

[25] FLUENT theory manual, "Turbulence Modeling, Section 10-7 [online]", Available at *http://www.shef.ac.uk/echeng/staff/xyl/fidap/help/theory/th10_03-08.htm#th1007*, [Last accessed 21 January (2006)].

[26] J.D. Anderson, Jr., Computational Fluid Dynamics, McGraw Hill, New York, USA (1995).

[27] E. Heinl and M. Bohent, "Calculation of Particle-Wall Adhesion in Horizontal Gas-Solid Flow Using CFD", Powder Tech., Vol. 159, pp. 95-104 (2005).

[28] Y. Tsuji, Y. Morikawa, T. Tanaka, N. Nakatsukasa, and M. Nakatani, "Numerical Simulation of Gas-Solid Two-Phase Flow in a Two Dimensional Horizontal Channel", Int. J. Multiphase Flow, Vol. 13 (5), pp. 671-684 (1987).

[29] M. Sommerfeld and N. Huber, "Experimental Analysis and Modeling of Particle-Wall Collisions ", Int. J. Multiphase flow, Vol. 25, pp. 1457-1489 (1999).

[30] S.V. Patankar, "Numerical Heat Transfer and Fluid Flow", McGraw-Hill, New York, U.S.A. (1983).

[31] C. Crowe, M. Sommerfeld and Y. Tsuji, Multiphase Flow with Droplets and Particles, CRC Press, Florida, U.S.A. (1998).

[32] M. Sommerfeld, "Particle Dispersion in a Plane Shear Layer ", 6 th Workshop on Two-Phase Flow Predictions, Erlangen, Germany (1992).

Received April 18, 2006
Accepted June 7, 2006